International Journal of Environmental Sciences
ISSN: 2229-7359
Vol. 11 No. 7, 2025
https://theaspd.com/index.php

Dual Solution of Axi-Symmetric Boundary Layer Flow and Heat Transfer Around a Stretching Cylinder Under the Influence of a Uniform Magnetic Field with Partial Slip Condition

Shefali Jauhri[1], **Upendra Mishra**[2]
[1]Department of Mathematics, Invertis University, Rajau Paraspur, National Highway NH 30, Bareilly, Uttar Pradesh 243123, Shefali.j@invertis.org
[2]Department of Mathematics, Amity University Rajasthan, NH-11 C, Kant Kalwar, Delhi-Jaipur Highway, Near Achrol Village, Jaipur, INDIA

Abstract
This study seeks to investigate the boundary layer flow of a viscous fluid possessing axisymmetric characteristics, where partial slip at the boundary is accounted for rather than assuming a no-slip condition. By employing similarity transformations, the governing equations transform. Subsequently, these transformed equations are numerically solved using the shooting method. The investigation uncovers the presence of dual solutions with increasing parameters such as velocity slip, magnetic field strength, and suction effect. Various physical parameters are meticulously examined and discussed. Furthermore, numerical analyses are performed to ascertain expressions for the skin friction coefficient, Nusselt number, fluid velocity, and temperature around the cylinder, with their variations elucidated through graphical representations.
Keywords: *Stretching cylinder, Dual solutions, Momentum slip condition, Thermal slip condition.*

1. INTRODUCTION:

Cylindrical slip flow refers to a specific type of fluid flow that occurs in cylindrical geometries, such as a pipe or a tube, where the flow is influenced by slip effects at the solid-fluid interface. When slip effects become significant, especially at the microscale, the behavior of a fluid flow can deviate from classical expectations. Slip flow can occur in situations where the mean free path of gas molecules is similar in magnitude to the characteristic length of the solid surface. Cylindrical slip flow has various applications in microfluidics, nanotechnology, and engineering at small scales. Understanding slip flow is essential for the design and optimization of microfluidic devices, where the effects of slip can significantly influence the performance and behavior of fluids in confined geometries. Researchers and engineers often use specialized models and computational simulations to analyze and predict slip flow behaviour accurately. In a groundbreaking study, in recent investigations, multiple researchers [1–4] have examined flow issues involving the inclusion of partial slip effects at the extending wall and the presence of a magnetic field introduces a novel aspect to the research. Adigun et al. [5] explore the motion of a viscoelastic nanofluid near a stagnation point under the influence of magnetohydrodynamics around an inclined cylinder undergoing linear stretching. Crane [6] explored the analysis of the flow arising from the stretching of a sheet. Datta et al. [7] proposed potential applications involving emergency shutdowns in nuclear reactors through cooling, where specific areas could be cooled by introducing a coolant. Ellahi et al. [8] explored the analysis of steady viscous liquid flow, incorporating a nonlinear slip condition, utilizing both analytic solutions and numerical solutions for flow analysis. Hayat et al. [9-10] investigated the colloidal properties of ferrofluid when subjected to a magnetic dipole and homogeneous and heterogeneous processes were also examined. Exploring the impact of magnets on horizontally and vertically elongated cylinders, Ishak et al. [11]. Ishak and Nazar [12] proposed the possibility of achieving similar solutions by considering the stretching cylinder with a linear velocity in the axial direction. Jagan [13] investigated Research into convective flow, which involves the transfer of heat and mass and has garnered significant attention due to its broad applications in numerous fields. This study delves into how The MHD flow around a stretching cylinder is influenced by nonlinearity in thermal radiation (NLTR), slip, as well as the effects of thermal diffusion (Soret) and diffusion-thermo (Dufour), with a focus on triple stratification (TSF). Jauhri S and Mishra U [14-16] studied the dual solution under 2nd -order slip boundary conditions. Lin and Shih [17-18] directed their attention to studying the smooth boundary layer and heat transfer around cylinders moving steadily, whether horizontally or vertically. They acknowledged the challenges in obtaining comparable results due to the influence of the cylinder's curvature.

International Journal of Environmental Sciences
ISSN: 2229-7359
Vol. 11 No. 7, 2025
https://theaspd.com/index.php

Mahapatra and Gupta [19] studied a two-dimensional viscous fluid system, exploring flow over an extended surface with heat transfer at a stagnation point. Mishra et. al [20] a study on the behavior of a viscous, incompressible fluid surrounding a vertically shrinking cylinder, focusing on heat transfer phenomena. In a separate investigation, Mukhopadhyay [21] analyzed how a uniform magnetic field affects the axisymmetric laminar boundary layer flow of a viscous, incompressible fluid moving towards a stretching cylinder, incorporating considerations of heat transfer. Mukhopadhyay [22] examined how partial slip affects the transfer of chemically reactive solutes over a stretching cylinder. Vinita et. al.,[23] explored the effects of magnetohydrodynamic slip flow combined with radiation on a nonlinear stretching cylinder, while considering the presence of an outer velocity. Mahmood [24] Given the promising applications of nanofluids, this research introduces a novel mathematical framework aimed at improving heat transfer by employing tri-hybrid nanofluids. The investigation examines the influence of heat generation/absorption and mass suction on magnetohydrodynamic (MHD) stagnation point flow over a nonlinearly stretching/shrinking sheet composed of a tri-hybrid nanofluid, with water as its base. Wang [25] researched describing the ongoing movement of a thick and unchanging fluid flowing around a stretching hollow cylinder within a motionless surrounding fluid. Yasmeen et. al [26] investigated the chemically reactive flow of ferrofluid. The occurrence of velocity slip, where the fluid doesn't adhere to a solid boundary, has been observed under certain conditions. The analysis of the results reveals a significant influence of magnetic and slip parameters on the flow field. Additionally, the study provides evaluations of heat transfer coefficients and skin friction coefficients, which are crucial considerations from an industrial application standpoint.

2. **Mathematical Formulation:** We considered an incompressible viscous fluid undergoes a continuous, axisymmetric flow along an elongating cylinder, influenced by a uniform magnetic field illustrated in Figure 1. The x-axis represents the cylinder's axis, and the r-axis extends radially. The assumption is made that there is a uniform magnetic field with intensity B_0 acting radially. To simplify, it's assumed that the magnetic Reynolds number is small, implying that the induced magnetic field is insignificant compared to the applied magnetic field. The governing equations for continuity, momentum, and energy in this particular flow scenario can be stated as follows:

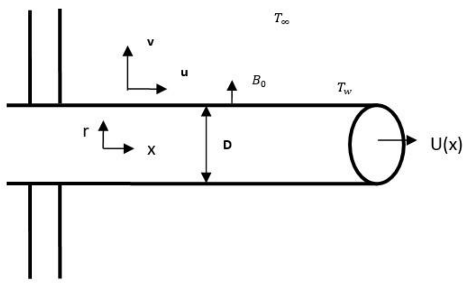

Fig.1.Illustration of the physical Model.

$$\frac{\partial(ru)}{\partial x}+\frac{\partial(rv)}{\partial r}=0 \quad (1)$$

$$u\frac{\partial u}{\partial x}+v\frac{\partial u}{\partial r}=\frac{\upsilon}{r}\frac{\partial}{\partial r}\left(r\frac{\partial u}{\partial r}\right)+g\beta_T(T-T_\infty)-\frac{\sigma B_0^2}{\rho}(u) \quad (2)$$

$$u\frac{\partial T}{\partial x}+v\frac{\partial T}{\partial r}=\frac{\kappa}{r}\frac{\partial}{\partial r}\left(r\frac{\partial T}{\partial r}\right) \quad (3)$$

Where u and v are the velocity components correspondingly aligned with the x-direction and r-direction, $\nu=\frac{\mu}{\rho}$ is the kinematic-viscosity, fluid density (ρ), dynamics fluid viscosity coefficient (μ), electrical conductivity (σ), uniform magnetic field (B_0), thermal-diffusivity (κ) of the fluid, fluid temperature (T).

3. **Boundary Conditions**

$$\left.\begin{array}{c} u=U+S_1\upsilon\frac{\partial u}{\partial r}+S_2\upsilon\frac{\partial^2 u}{\partial r^2} \\ v=0 \\ T=T_w+q_1\frac{\partial T}{\partial r}\end{array}\right\}\text{at } r=D \quad (4)$$

$$\left.\begin{array}{c} u\to 0 \\ T\to T_\infty\end{array}\right\}\text{at } r\to\infty \quad (5)$$

In reference of velocity, S_1 and S_2 are slip parameters and kinematic-viscosity is 'ν'. Here q_1 temperature slip parameters in reference of temperature and concentration. $U=cx$, is the stretching velocity for $c=$

1 and shrinking velocity for $c = -1$ is the prescribed surface temperature. The continuity equation is fulfilled by incorporating the stream function ψ as $u = \frac{1}{r}\frac{\partial\psi}{\partial r}$ and $v = -\frac{1}{r}\frac{\partial\psi}{\partial x}$.

4. Coefficient of Skin friction

The skin-friction coefficient at the cylinder's surface is defined as

$$\frac{1}{2}\sqrt{Re}C_f = f''(0)$$

5. Coefficient of Nusselt number

The heat transfer rate, represented by the Nusselt number, at the cylinder's surface is defined as

$$\frac{Nu}{\sqrt{Re}} = -\theta'(0)$$

6. Method of Solution:

Introducing the similarity variables as,

$$\xi = \frac{r^2-R^2}{2R}\left(\frac{U}{\nu x}\right)^{1/2}, \quad \psi = (U\upsilon x)^{\frac{1}{2}}Rf(\xi), \quad \theta(\xi) = \frac{T-T_\infty}{T_w-T_\infty}$$

$$u(\xi, r) = Uxf'(\xi), \quad v(\xi, r) = -\frac{R}{r}\sqrt{U\nu}f(\xi) \tag{6}$$

$$(1+2K\xi)h''' + (2K+h)h'' - h'^2 - Me^2h'' - \gamma t = 0 \tag{7}$$

$$(1+2K\xi)t'' + 2Kt' + P_r(ht' - h't) = 0 \tag{8}$$

Boundary Conditions

$$\left.\begin{aligned} h(\xi) = S, h'(\xi) = a + \beta_1 h''(\xi) + \beta_2 h''(\xi) \\ \theta(\xi) = 1 + \delta_1 t'(\xi) \end{aligned}\right\} \text{at } \xi = 0 \tag{9}$$

$$\left.\begin{aligned} h'(\xi) \to 0 \\ h(\xi) \to 0 \end{aligned}\right\} \text{at } \xi \to \infty. \tag{10}$$

Where $\beta_1 = S_1\sqrt{\frac{\nu U_0}{L}}$ and $\beta_2 = S_2\frac{U_0}{L}$, $a = (> 0/< 0)$ for stretching/ shrinking cylinder, $a = 0$ for static-cylinder and are referred to as the 2nd and 3rd order coefficients of slip parameters. $\delta_1 = q_1\sqrt{\frac{U_0}{\nu L}}$ are referred to as the slip coefficient of heat transfer. The curvature parameter $K = \sqrt{\frac{\nu}{UR^2}}$, Buoyancy parameter $\gamma = \frac{g\beta_T(T_w-T_\infty)}{U^2x}$, Prandtl number $P_r = \frac{\nu}{\alpha}$, Reynold number $Re = \frac{U_0x}{\nu}$.

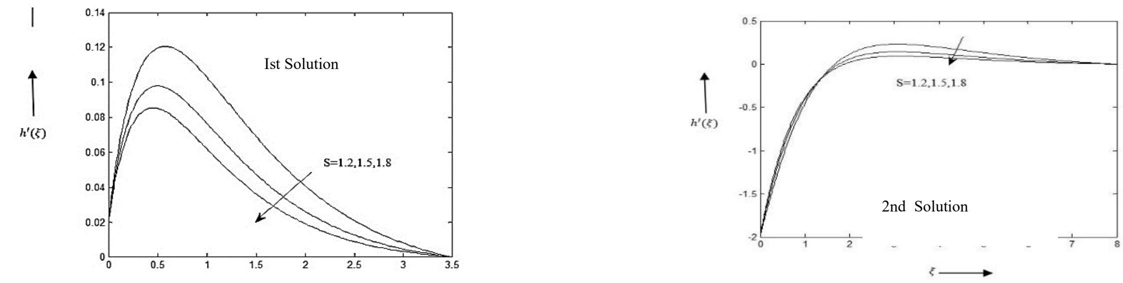

(a) (b)

Fig.2(a) and 2(b) variation of velocity parameter h' vs ξ across various values 's' when $\beta_1 = 0.1, \beta_2 = 0.1, \delta_1 = 0.1, K = 0.1, M_e = 0.1$ for the Ist and 2nd solution.

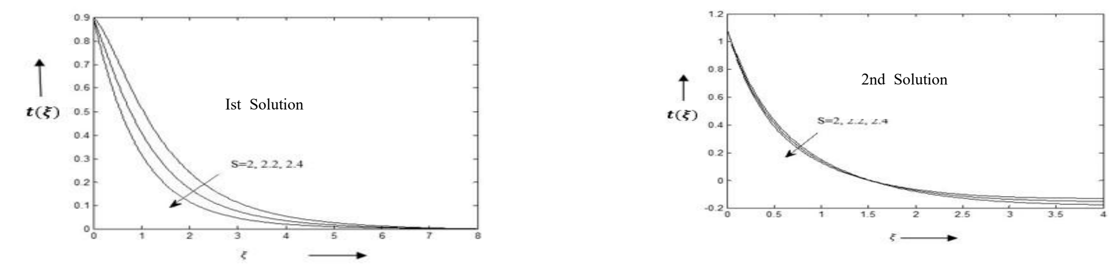

(a) (b)

Fig.3(a) and 3(b) variation of temperature parameter t vs ξ across various values 's' when $\beta_1 = 0.1, \beta_2 = 0.1, \delta_1 = 0.1, K = 0.1, M_e = 0.1$ for the Ist and 2nd solution.

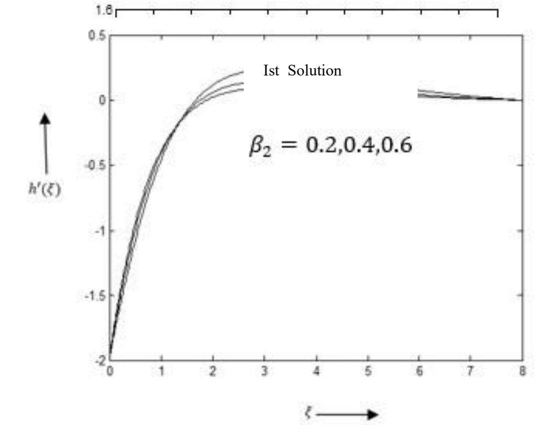

2nd Solution

(a) (b)

Fig.4(a) and 4(b) variation of velocity parameter $h'(\xi)$vs ξ across various values 's' when $\beta_1 = 0.1, s = 0.1, \delta_1 = 0.1, K = 0.1, M_e = 0.1$ for the Ist and 2nd solution.

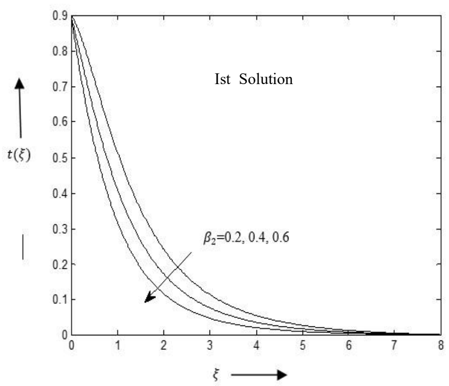

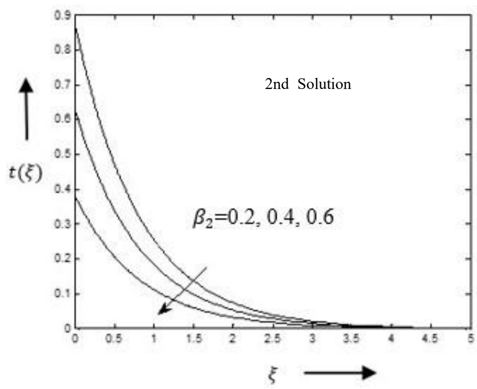

(a) (b)

Fig.5(a) and 5(b) variation of velocity h' vs parameter ξ across various values 'β_2' when $\beta_1 = 0.1, s = 0.1, \delta_1 = 0.1, K = 0.1, M_e = 0.1$ for the Ist and 2nd solution.

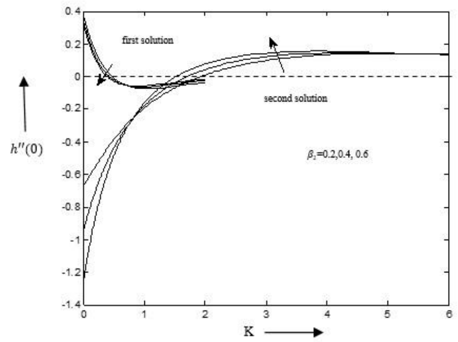

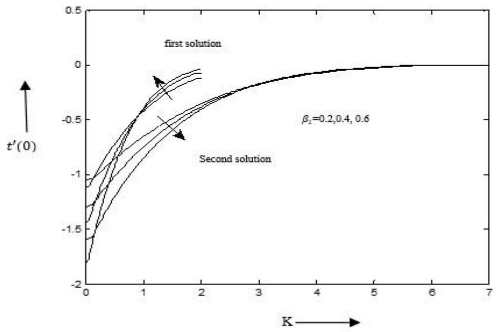

(a) (b)

Fig.6 is variations of stream function $h''(0)$ and fig.7 is variations of $t'(0)$ vs parameter K across various values 'β_2' when $\beta_1 = 0.1, s = 0.1, \delta_1 = 0.1, K = 0.1, M_e = 0.1$ for the Ist and 2nd solution.

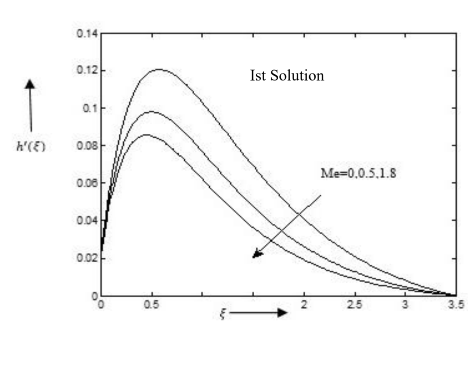

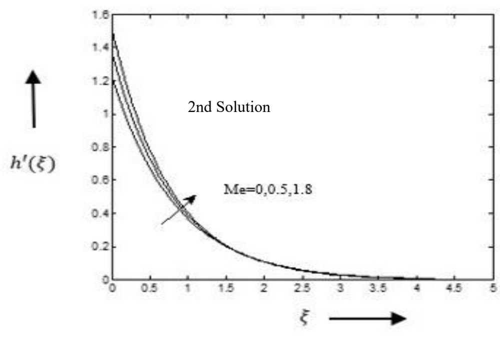

(a) (b)

Fig.8(a) and 8(b) are variations of velocity parameter $h'(\xi)$ vs ξ parameter across various values 'M_e' when $\beta_1 = 0.1, \beta_2 = 0.1, s = 0.1, \delta_1 = 0.1, K = 0.1$ for the Ist and 2nd solution.

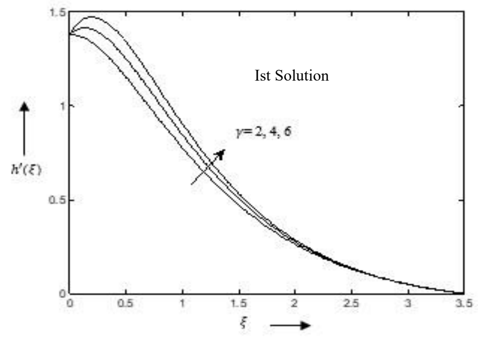

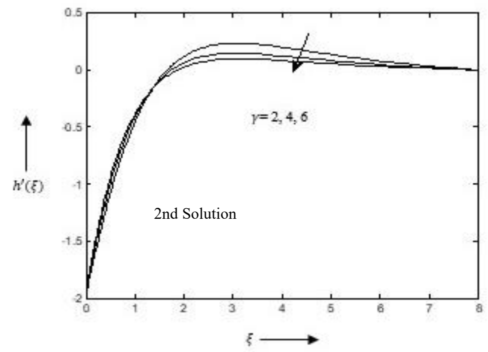

(a) (b)

Fig.9(a) and 9(b) are variations of velocity parameter $h'(\xi)$ vs ξ parameter across various values 'γ' when $\beta_1 = 0.1, \beta_2 = 0.1, s = 0.1, \delta_1 = 0.1, K = 0.1, s = 0.1$ for the Ist and 2nd solution.

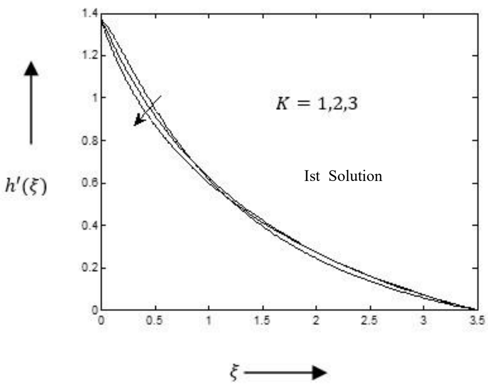

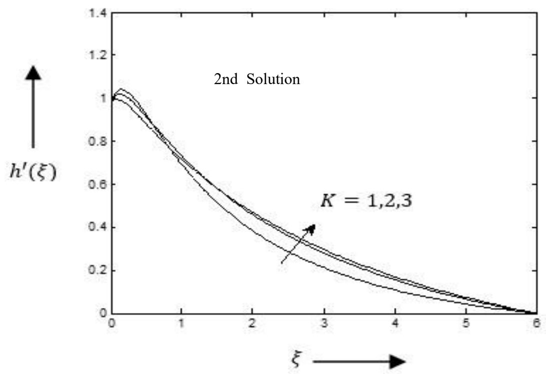

(a) (b)

Fig.10(a) and 10(b) are variations of velocity parameter $h'(\xi)$ vs ξ parameter across various values 'K' when $\beta_1 = 0.1, \beta_2 = 0.1, s = 0.1, \delta_1 = 0.1, K = 0.1, s = 0.1$ for the Ist and 2nd solution.

Table 1:- The values of $-t'(0)$ are determined for various temperature exponent values n on a flat plate (where K=0) under conditions of zero magnetic field (Me =0) and Prandtl number (P_r) equal to 1.

n	Ishak and Nazar	Mukopadhyay S	Present Study
0	0.5820	0.5821	0.5821
1	1.0000	1.0000	1.0000
2	1.3333	1.3332	1.3334

Table 2:-Values of $[-h''(0)]$ and $[-t'(0)]$ for several values of curvature parameter K and magnetic parameter Me with Pr=1,n=1.

Me	K	$-h''(0)$	$-t'(0)$
0	0.1	1.2902	0.8927
0.2	0.1	1.3123	0.8875
0.4	0.1	1.3760	0.8728
0.6	0.1	1.4755	0.8505

0.1	0	-1.2529	-0.8533
0.1	0.2	-1.3387	-0.9307
0.1	0.4	-1.4241	-1.0090
0.1	0.6	-1.5084	-1.0859

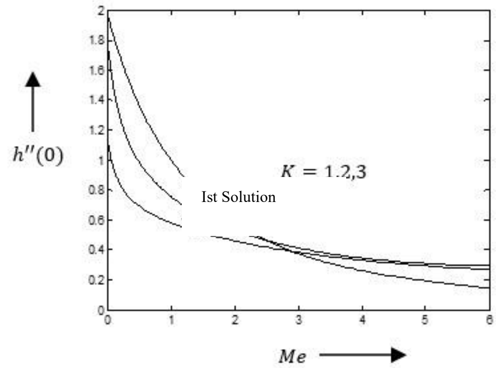

2nd Solution

(a) (b)

Fig.11(a) and 11(b) are variations of velocity parameter $h''(0)$ vs Me across various values 'K' when $\beta_1 = 0.1, \beta_2 = 0.1, s = 0.1, \delta_1 = 0.1, s = 0.1$ for the Ist and 2nd solution.

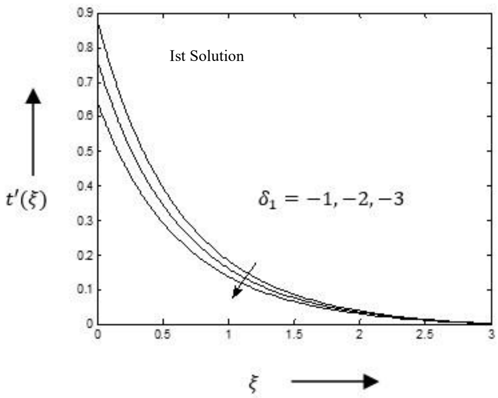

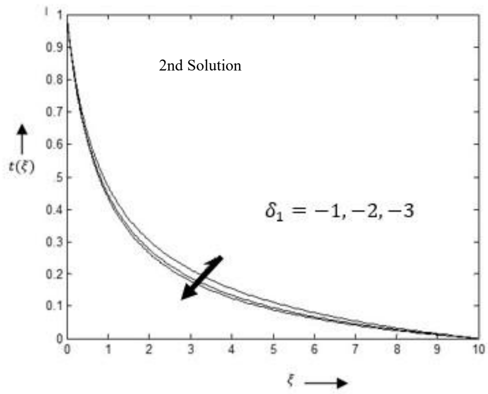

(a) (b)

Fig.12(a) and 12(b) are variations of velocity parameter $t'(\xi)$ vs ξ parameter across various values 'δ_1' when $\beta_1 = 0.1, \beta_2 = 0.1, K = 0.1, s = 0.1$ for the Ist and 2nd solution.

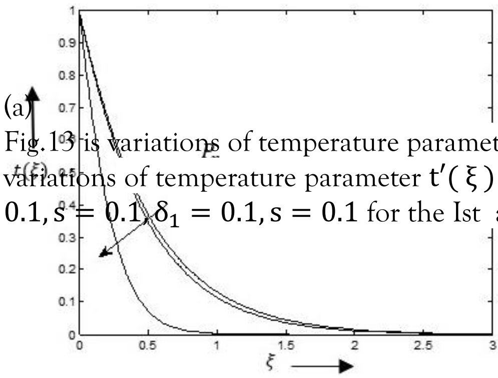

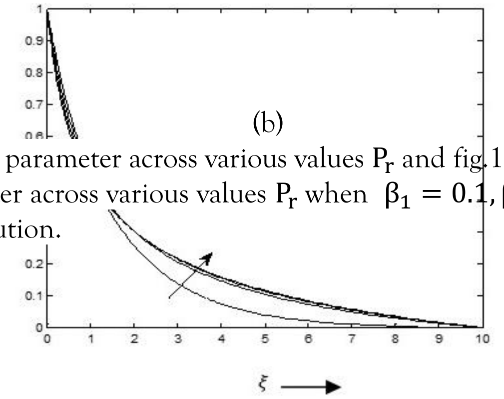

(a) (b)

Fig.13 is variations of temperature parameter $t'(\xi)$ vs ξ parameter across various values P_r and fig.14 are variations of temperature parameter $t'(\xi)$ vs ξ parameter across various values P_r when $\beta_1 = 0.1, \beta_2 = 0.1, s = 0.1, \delta_1 = 0.1, s = 0.1$ for the Ist and 2nd solution.

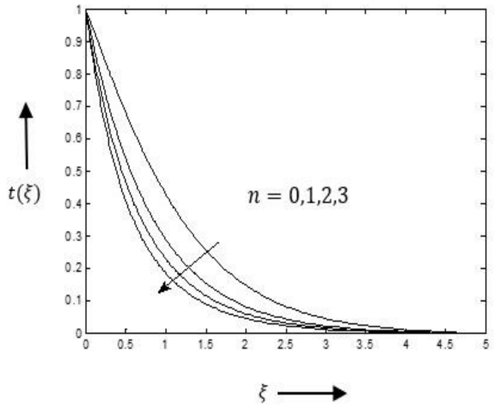

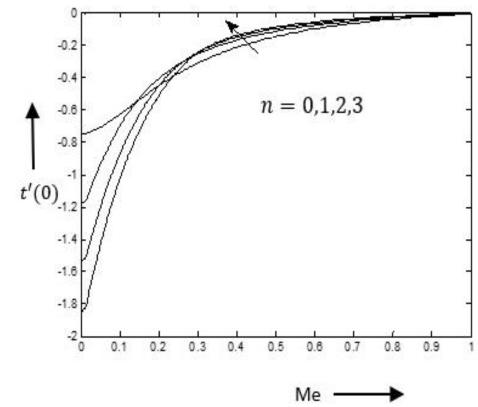

(a) (b)

Fig.15 is variations of temperature parameter $t(\xi)$ vs ξ and fig. 16 is variations of $t'(0\xi)$ vs ξ across various values 'n' when $\beta_1 = 0.1, \beta_2 = 0.1, s = 0.1, \delta_1 = 0.1, K = 0.1, s = 0.1$ for the Ist and 2nd solution.

7. RESULT AND DISCUSSION

Equations (7) and (8) and their associated boundary conditions (9) have been solved using numerical methods. The analysis reveals the existence of two separate solutions within the system. To assess the accuracy of the numerical method used, we compared our current results for the heat transfer coefficient (-t'(0)) under specific conditions: no-slip conditions, absence of a magnetic field (Me = 0), and a flat stretching plate (K = 0), with those reported by Ishak and Nazar [17] and Mukhopadhyay S. These comparisons are summarized in Table 1, showing close agreement with previous studies. Additionally, Table 2 presents numerical data for the stretching cylinder incorporating 2nd -order slip boundary conditions.Figures 2(a, b) and 3(a, b) depict a decline in both fluid velocity and temperature as s increases. Additionally, a decrease in the thickness of the velocity boundary layer is noted with increasing s, aligning with the concept that boundary layer thickness diminishes with heightened suction. Conversely, in the 2nd solution, both velocity and thermal boundary layer thicknesses are larger compared to the Ist solution, and the velocity boundary layer thickness does not diminish with an increase in s.In Fig. 4(a), it's evident that the fluid velocity rises as β_2 increases, suggesting a positive correlation between these variables. Conversely, Fig. 4(b) indicates a decrease in fluid velocity with increasing β_2. This contrasting trend might arise from varying conditions or factors affecting the system. Moving on to Fig. 5(a & b), both subfigures illustrate a decline in fluid temperature as $\beta_2$increases. This inverse relationship implies that as β_2, increases, the fluid temperature tends to decrease. These observations provide valuable insights into the dynamics of the system under study, highlighting the interplay between fluid velocity, temperature, and the parameter β_2. Figure 6 shows that as β_2 increases $f''(0)$ decreases, whereas for the 2nd solution, it increases. In Figure 7, the influence of β_2 on $-t'(0)$ is observed to increase in the Ist solution; however, for the 2nd solution, it decreases. As the parameter Me increases, a noticeable trend emerges where the velocity experiences a decrease, as illustrated in Figures 8(a) while increases in 2nd solution as shown in Fig. 8(b). This behavior persists up to specific heights, after which the deceleration process becomes more gradual. The magnetic parameter Me plays a significant role in shaping the results, suggesting that the existence of a magnetic field imposes more restrictions on the fluid, leading to a decrease in fluid velocity. Observations from Fig. 9(a, b) for the Ist solution indicate that as the buoyancy parameter γ increases, h' increases, while decreases in 2nd solution. Concerning the 2nd solution, it's noted that as γ increases, the domain of existence for the 2nd solution expands. Ist , let's explore the impact of the curvature parameter K on the velocity distribution under a magnetic field.Figures 10(a & b) depict velocity profiles h'(ξ) for different K values. Across all cases, the velocity reaches zero at a noticeable distance. In the Ist solution, velocity decreases as the curvature parameter K increases, while in the 2nd solution, it increases. Regarding the temperature profile (Fig. 14), after reaching a certain distance, it begins to increase with increasing K values. The transverse curvature parameter serves as an indicator of a cylinder's geometric property. An increase in the transverse curvature parameter K signifies a reduction in the cylinder's radius, indicating that the cylinder is becoming slimmer or more slender. In Figures 11(a & b), higherK values lead to lower $h''(0)$ for the Ist solution, while the 2nd solution exhibits a higher skin-friction coefficient. Figures 12(a, b) show that as the temperature slip parameter δ_1 increases, temperature decreases in both cases. Figure 13 demonstrates that as the Prandtl number increases, fluid temperature decreases. Moreover, the thermal boundary layer thickness decreases with an increase in the Prandtl number. The temperature rises with n, yet there is no observed temperature overshoot for the cylinder as depicted in figure 15. It is observed in figure 16 that elevating n results in an augmentation of the local Nusselt number.

CONCLUSION:-

A numerical investigation into the boundary layer flow along a stretching cylinder has been carried out. The study reveals two distinct solutions: the Ist and 2nd solutions. Notably, the domain where the 2nd solution is applicable varies with changes in the physical parameter. It is worth mentioning that for the Ist solution, the profiles of h'(ξ) and t(ξ) tend to converge as suction varies. This Ist solution leads to reduced velocity and thermal boundary layer thicknesses. Furthermore, in this Ist solution, the velocity boundary layer thickness decreases with increasing suction parameter, indicating its practical relevance. However, the 2nd solution is primarily a mathematical artifact resulting from the nonlinearity of the model and does not exhibit consistent trends with changes in physical parameters. Nonetheless, apart from the slip parameter (Ist -order), the temperature profiles of both the Ist and 2nd-order solutions show similar trends as the physical parameters vary. Additionally, geometric parameters such as the curvature parameter and Prandtl number influence fluid and temperature profiles.

8. REFERENCES: -

1. Andersson H.I., (2002): Slip flow past a stretching surface. Acta Mech; vol.158, pp.121–126.
2. Ariel P.D., Hayat T, Asghar S, (2006): The flow of an elasticoviscous fluid past a stretching sheet with partial slip. Acta Mech, vol.187, pp.29–35.
3. Ariel P.D., (2008): Two-dimensional stagnation point flow of an elasticoviscous fluid with partial slip. ZAMM Journal of Applied Mathematics and mechanics, vol.88, pp.320–324.
4. Abbas Z, Wang Y, Hayat T, Oberlack M. (2009): Slip effects and heat transfer analysis in a viscous fluid over an oscillatory stretching surface. Int J Numer Meth Fluids, vol. 59, pp.443–58.
5. Adigun J.A, Adeniyan A, Abiala I.O,(2021): Stagnation point MHD slip-flow of viscoelastic nanomaterial over a stretched inclined cylindrical surface in a porous medium with dual stratification. International Communications in Heat and Mass Transfer, Vol. 126, pp. 1-16, https://doi.org/10.1016/j.icheatmasstransfer.2021.105479
6. Crane L.J. (1970): Flow past a stretching plate., J. Appl. Math. Phys. (ZAMP), vol.21, pp.645-647.
7. Datta B.K., Roy P., Gupta A. S., (1985): Temperature field in the flow over a stretching sheet with uniform heat flux, Int Commun Heat Mass Transfer, vol.12, pp.89–94.
8. Ellahi R., Hayat T., Javed T., Asghar S., (2008): On the analytic solution of nonlinear flow problem involving Oldroyd 8-constant fluid, Mathematical and Computer Modelling, 48(8), pp. 1191-1200 DOI: 10.1016/j.mcm.2007.12.017.
9. Hayat T, Abbas Z, Sajid M., (2006): Series solution for the upper convected Maxwell fluid over a porous stretching plate. Phys Lett A, vol.358, pp.396–403.
10. Hayat T, Sajid M. (2007): Analytic solution for axisymmetric flow and heat transfer of a 2nd-grade fluid past a stretching sheet. Int J Heat Mass Transfer, vol.50, pp.75–84.
11. Ishak A, Nazar R, Pop I. (2008): Uniform suction/blowing effect on flow and heat transfer due to a stretching cylinder. Appl Math Modell, vol.32, pp.2059–2066.
12. Ishak A, Nazar R.(2009): Laminar boundary layer flow along a stretching cylinder. Eur J Sci Res, vol.36(1), pp.22–29.
13. Jagan, K., Sivasankaran, S., (2022): Soret & Dufour and Triple Stratification Effect on MHD Flow with Velocity Slip towards a Stretching Cylinder. Math. Comput. Appl., 27(25), pp.1-15 . https://doi.org/10.3390/mca27020025
14. Jauhri S, Mishra U., (2021): Dual Solutions of EMHD Nanofluid at Stretching Sheet with Mixed Convection Slip Boundary Condition, Int. J. of Heat and Technology., 39(6), pp. 1887-1896.
15. Jauhri S, Mishra U., (2023): Numerical investigation of MHD nanofluid considering 2nd -order velocity slip effect over a stretching sheet in porous media, Journal of Integrated Science and Technology., 11(2), pp. 478-485.
16. Jauhri S, Mishra U., (2022): A study of MHD fluid with 2nd-order slip and thermal flow over a nonlinear stretching sheet, Int. J. of Applied Mechanics and Engineering., 27(2), pp. 98-114.
17. Lin H.T., Shih Y.P., (1980): Laminar boundary layer heat transfer along static and moving cylinders. J Chin Inst Eng, vol.3, pp.73–79.
18. Lin H.T., Shih Y.P., (1981): Buoyancy effects on the laminar boundary layer heat transfer along vertically moving cylinders. J Chin Inst Eng, vol.4, pp.47–51.
19. Mahapatra T, Gupta A. S.,(2004): Stagnation-Point Flow of a Viscoelastic Fluid Towards a Stretching Surface, International Journal of Non-Linear Mechanics 39(5):811-820 DOI: 10.1016/S0020-7462(03)00044-1.
20. Mishra U., Singh G., (2014): Dual solutions of mixed convection flow with momentum and thermal slip flow over a permeable shrinking cylinder, Computers & fluids, Vol.93, pp.107-115, https://doi.org/10.1016/j.compfluid.2014.01.012.
21. Mukhopadhyay S., (2013):MHD boundary layer slip flow along a stretching cylinder, Ain Shams Engineering Journal, Vol 4(2), Issue 2, Pp. 317-324, https://doi.org/10.1016/j.asej.2012.07.003.
22. Mukhopadhyay S., (2011): Chemically reactive solute transfer in a boundary layer slip flow along a stretching cylinder. Front Chem Sci Eng;5(3):385–91. http://dx.doi.org/10.1007/s11705-011-1101-4.
23. Vinita, Kumar Parveen, Poply Vikas, (2023): Mathematical Modelling of Magnetohydrodynamic Nanofluid Flow with Chemically Reactive Species and Outer Velocity Towards Stretching Cylinder, Journal of Nanofluids, vol. 12(4), pp.1067-1073.

24. Mahmood Z., Eldin S.M., Rafique K., Khan U.,(2023): Numerical analysis of MHD tri-hybrid nanofluid over a nonlinear stretching/shrinking sheet with heat generation/absorption and slip conditions, Alexandria Engineering Journal, VoL.76,pp. 799-819, https://doi.org/10.1016/j.aej.2023.06.081.
25. Wang CY. Flow due to a stretching boundary with partial slip – an exact solution of the Navier–Stokes equations. Chem Eng Sci 2002; 57: 3745–7.
26. Yasmeen T., Hayat T., Khan M., Imtiaz M., Alsaedi A., 2016: Ferrofluid flow by a stretched surface in the presence of magnetic dipole and homogeneous-heterogeneous reactions, Journal of Molecular Liquids 223., DOI: 10.1016/j.molliq.2016.09.028